Effects of the relative contents of silver and copper on the interfacial reactions and bond strength in the active brazing of SiC

HYOUNG-KEUN LEE*, SUN-HYO HWANG*, JAI-YOUNG LEE
Korea Advanced Institute of Science and Technology, P.O. Box 150, Cheongyang, Seoul, Korea

The roles of titanium in active brazing of SiC have been studied extensively, while studies on the roles of silver and copper, which constitute the major parts of the active brazing alloys, have been overlooked. The effects of the relative contents of silver and copper in the brazing alloy on the interfacial reactions and bond strength have been investigated in this study. The interfacial reactions can be divided into the decomposition reaction of SiC by the brazing alloy melt and the interfacial reaction of titanium with SiC. Brazing by the Cu–5 at % Ti alloy induced SiC to be decomposed, but the addition of silver to the brazing alloy suppressed the decomposition of SiC. TiC and Ti_5Si_3 was produced from the interfacial reactions of titanium independent of the brazing alloys. However, their morphologies and formation mechanisms differ greatly depending on the relative contents of silver and copper. The bond strength and fracture modes are also dependent on the relative contents of silver and copper. A good bond strength of 159–178 MPa was obtained by brazing with the Ag–5 at % Ti alloy at 985 °C for 600 s and fracture initiates at the interface of the reaction product layer and propagates through SiC.

1. Introduction

Structural and other applications of silicon carbide (SiC) have been expected because of its good high-temperature strength, wear resistance, and anticorrosion characteristics. But there are many cases in which the technology to bond SiC to itself or to metals is required for practical applications [1, 2]. The brazing process among the various bonding methods, is the most promising for practical applications. To be used as brazing alloys, alloys should have the appropriate wettability and good bond strength to SiC. Most of the brazing research on SiC has been conducted using a silver–copper eutectic alloy with 2–6 wt % titanium because it has good wettability to the ceramic, a low melting point, and high ductility [3]. The use of an Ag–Cu–Ti alloy involves interfacial reactions with ceramics during brazing. The bond strength between SiC and a brazing alloy is affected by the microstructure of the reaction products at the interface. The interfacial reaction mechanism and the relationship between the bond strength and the microstructure of the reaction products should be identified to obtain a braze joint with high bond strength. The roles of titanium on the wetting, interfacial reactions and bond strength in the active brazing of SiC by an Ag–Cu–Ti alloy have been the major object of recent research [4, 5]. However, the effects of silver and copper, which constitute the major parts of a brazing alloy, on the interfacial reactions, have not been studied extensively. Silver and copper belong to the same group in the Periodic Table and have similar chemical properties. They can hardly form silicides and carbides because the d electron shell structure is filled. The activity of silicon in the silver and copper melt is very different [6, 7], which can heighten the difference in interfacial reactions according to the relative contents of silver and copper in the brazing alloy. Gnesin and Naidich [8] reported the formation of siliceous phases from the reaction between SiC and the copper melt. It is believed that the relative content of silver and copper in the brazing alloy affects the interfacial reactions. In this study, the effects of the relative content of silver and copper on the interfacial reactions and bond strength were analysed. The microstructure was analysed by scanning electron microscopy (SEM), energy dispersive X-ray spectroscopy (EDX), and X-ray diffractometry (XRD) using a copper target. The bond strengths were evaluated by four-point bend tests.

2. Experimental procedure

SiC was pressurelessly sintered to the size of 12.5 mm × 12.5 mm × 5 mm and contained 1–2 wt % free carbon and about 3 vol % porosity. The brazing alloys were prepared by precise weighing and mixing of silver, copper and titanium powder that have a purity

---

TABLE I Brazing alloys and brazing conditions used in this study

	Ag (at %)	Cu (at %)	Ti (at %)	Brazing conditions	
				Temp. (°C)	Time (s)
1	–	95	5	1100	600, 3600
2	95	–	5	985	600
				1100	600
3	57	38	5	830	600, 1800
				920	600
4	35	60	5	890	600
5	76	19	5	980	600
6	9.5	85.5	5	1100	600

Figure 2 Preparation procedure of the specimens for the four-point bend tests. (a) Brazing, (b) cutting, (c) polishing.

Figure 1 Schematic diagram of a vacuum furnace used in this study. 1, Specimen; 2, graphite heating element; 3, water-cooled copper electrode; 4, Pt–Rd thermocouple; 5, heat shield box; 6, vacuum chamber; 7, cooling coils; 8, viewing port; 9, telescope and camera; 10, to vacuum system.

of 99.0 wt %. The compositions of the brazing alloys were selected as copper, silver and Ag_xCu_y alloy with 5 at % Ti and are shown in Table I. The brazing experiments were conducted at the temperature which had approximately a 40° wetting angle, which was measured during the heating cycle, and at a temperature that had a fully liquid phase from the two- and three-component phase diagram [9]. The brazing conditions are also listed in Table I.

Before brazing, the SiC blocks were polished with 6 μm diamond paste and ultrasonically cleaned in acetone solution. To keep the brazing gap constant, a 0.2 mm diameter tungsten wire, used as a spacer, was inserted with the brazing alloy between the SiC blocks. To measure the wetting angles, a prepacked brazing alloy of 5 mm diameter × 5 mm thick disc shape was placed on the SiC block.

The brazing and wetting angle measurements were carried out in a vacuum furnace. A schematic diagram of the vacuum furnace is shown in Fig. 1. The specimens (1) are heated at the rate of 6.7 °C min^{-1} by a graphite heating element (2). Temperature is measured by a Pt–Rd thermocouple (4) which is placed in contact with the SiC block. The specimens are cooled at the rate of 6 °C min^{-1} to 600 °C and 3 °C min^{-1} to room temperature. The heating and cooling rates are controlled in the range ± 1 °C by a programmable controller. A vacuum of ~ 10^{-5} torr (1 torr
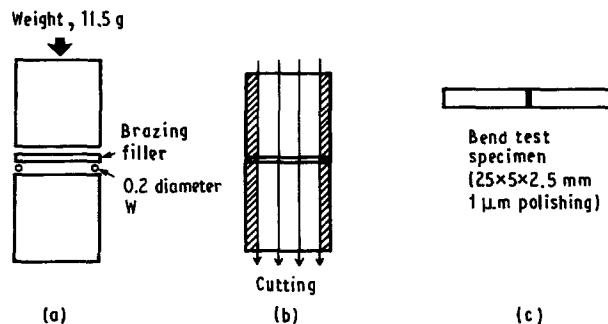
= 133.322 Pa) is maintained until melting of the brazing alloy occurs. For wetting angle measurements, a telescope and a camera (9) are installed at the viewing port (8) of the furnace.

The preparation procedure of the specimens for the four-point bend tests is shown schematically in Fig. 2. Both sides of the brazement were removed and the centre parts were sliced to the size 5 mm × 2.8 mm × 25 mm by a low-speed diamond saw. All the specimens were polished to 1 μm diamond paste. The specimens without any microcracks when observed by optical microscopy were used for the bend tests. The four-point bend tests were carried out using an Instron universal testing machine with a special jig that has an inner span of 6 mm and an outer span of 18 mm. The crosshead speed was 0.5 mm min^{-1}. The results were evaluated from at least three measured values.

3. Results
3.1. Measurement of wetting angles

It is generally known that the wetting of metals to ceramics is difficult, but the addition of 2–6 wt % titanium can improve wettability greatly. It seems that the improvement is related to an interfacial reaction of titanium [10, 11]. However, some researchers [12] insist that titanium adsorption at the interface improves wettability. When a chemical reaction at the interface is involved, the wetting mechanism is very complicated and not yet well known.

From the practical point of view, the wetting behaviour of a brazing alloy affects penetration of the melt into the brazing gap and the formation of defects. A brazing alloy should have good wettability to be applied. Moorhead and Keating [13] mentioned that a wetting angle of about 70° or less is satisfactory to braze ceramics. In this research, wetting angles were measured to determine the wetting characteristics according to the relative contents of silver and copper, to judge the suitability as a brazing alloy, and to decide the brazing temperature range. Fig. 3 shows the results of wetting angle measurements for the Cu–5 at % Ti, Ag–5 at % Ti and $Ag_{0.6}Cu_{0.4}$–5 at % Ti alloy during the heating cycle. The wetting angles with the Cu–5 at % Ti alloy decreased slowly with increasing temperature. A wetting angle of about 40° was obtained at 1100 °C. The equilibrium wetting angle measured after 3600 s at 1100 °C was 35°–40° and
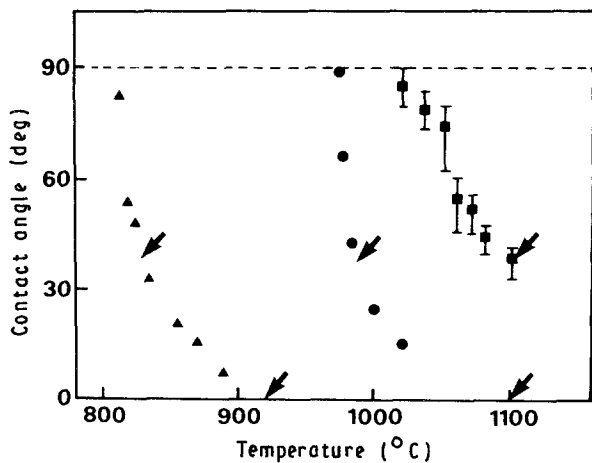
Figure 3 Wetting angles measured during heating at the rate of 6.7 °C min⁻¹. Arrows indicate the brazing temperatures for each brazing alloy.

almost equal to that measured during the heating cycle. The brazing temperature was selected as 1100 °C because the brazing alloy fully enters a liquid phase and has a proper wetting angle. In the Ag–5 at % Ti alloy, the wetting angles decreased steeply with temperature from 975 °C at which the brazing alloy exists as partial liquid state, and have a value lower than 5° at 1050°C. The silver component vaporized after melting the brazing alloy. It appears that the vaporization contributes to the lowering of the wetting angles. The brazing temperatures were selected as 985°C, at which the brazing alloy has a wetting angle of about 40°, and 1100 °C at which the brazing alloy is in a liquid state and the brazing temperature is equal to that of the Cu–5 at % Ti alloy. The equilibrium wetting angle measured after 3600 s at 985 °C was about 16°. The wetting angles in the $Ag_{0.6}Cu_{0.4}$–5 at % Ti alloy rapidly decreased with temperature from 815 °C and spread out at about 910 °C. The brazing temperatures were selected as 830 and 920 °C in the same way as other brazing alloys. The equilibrium wetting angle at 830 °C was less than 5°. The $Ag_{0.8}Cu_{0.2}$–5 at % Ti and $Ag_{0.37}Cu_{0.63}$–5 at % Ti alloy showed good wetting behaviour similar to the $Ag_{0.6}Cu_{0.4}$–5 at % Ti alloy.

The wetting behaviour changes with the relative contents of silver and copper in the brazing alloy. The Cu–5 at % Ti alloy has a little difficulty in wetting SiC and the wetting behaviour seems to be closely related to the decomposition reaction of SiC. The Ag–5 at % Ti and Ag_xCu_y–5 at % Ti alloys are able to wet SiC easily. However, it seems that the vaporization of the silver component in the Ag–5 at % Ti alloy contributes to the decreasing wetting angles. Because the detailed wetting mechanism for each alloy will be complicated, further research is required to understand it.

3.2. The microstructures at the interface
3.2.1. Cu–5 at % Ti alloy

Fig. 4 shows the microstructure and element distributions by EDX at the interface of the specimen brazed at 1100 °C for 600 s. The reaction zone has a thickness

of about 30 μm and can be divided into three reaction layers. Reaction layers I and II extend to the SiC side from the original interface. Carbon, copper and silicon are located mainly in layer I, titanium and carbon in layer II, and titanium and silicon in layer III. After grinding SiC parallel to the braze joint, XRD analysis was conducted on the ground surface which was composed of the reaction layers. Fig. 5a shows the results of XRD analysis. Graphite, Cu_7Si and TiC were identified as the reaction products. A small amount of copper phase remained in the layers. Comparing the element distributions, layer I is composed of graphite and Cu_7Si, and layer II of TiC and a small amount of Cu_7Si. Layer III is too thin to be detected in this XRD analysis, but it has been ascertained in a previous paper [14] that this layer is composed of the Ti_5Si_3 phase. Reaction layer I was formed due to the decomposition of SiC by the copper melt. Fig. 5b shows the result of XRD analysis which was carried out on the brazing alloy surface. A quantitative analysis by EDX shows that the brazing alloy matrix is composed of 85.8 Cu, 14.0 Si and 0.2 at % Ti. The result implies that the brazing alloy matrix has completely changed to the Cu_7Si phase. It is known that the brazing alloy matrix is gradually changed from copper to Cu_7Si and Cu_5Si, depending on the extent of the decomposition reaction [14]. Titanium silicide particles are distributed in the brazing alloy matrix.

Fig. 6 shows the reaction layers on the specimen wetted for 3600 s, observed after removing the brazing alloy by deep etching and cleaning ultrasonically in acetone. The particles (A) are the Ti_5Si_3 phase in reaction layer III and have been grown in a hexagonal pillar shape reflecting its crystal structure. Layer B corresponds to reaction layer II. Layer C displays the skeleton of graphite in reaction layer I. (D) corresponds to the SiC matrix.

3.2.2. Ag–5 at % Ti alloy

Fig. 7 shows the microstructure and line analysis for elements by EDX at the interface brazed by the Ag–5 at % Ti alloy. The reaction zone was different from the case of the Cu–5 at % Ti alloy and was composed of two layers. One was the thin layer I in contact with the SiC and the other was layer II, having the shape of a sparse band in the side of the brazing alloy matrix. The decomposition of SiC did not occur in this brazement. The reaction layers brazed at 985 °C did not differ much from those at 1100 °C. At higher temperatures, layer I became a little thicker and the dark region of the band in layer II became denser. The element distributions in Fig. 7b show that titanium and carbon have a peak in layer I, while layer II contains titanium and silicon. The white region of the band in layer II is composed of silver. Fig. 8 shows the results of XRD analysis for the reaction layers after grinding out the brazing alloy matrix parallel to the braze joint. TiC and Ti_5Si_3 were observed as reaction products. From the element distributions and XRD analysis, layer I was composed of the TiC phase and the dark region of the band, layer II, the Ti_5Si_3 phase.
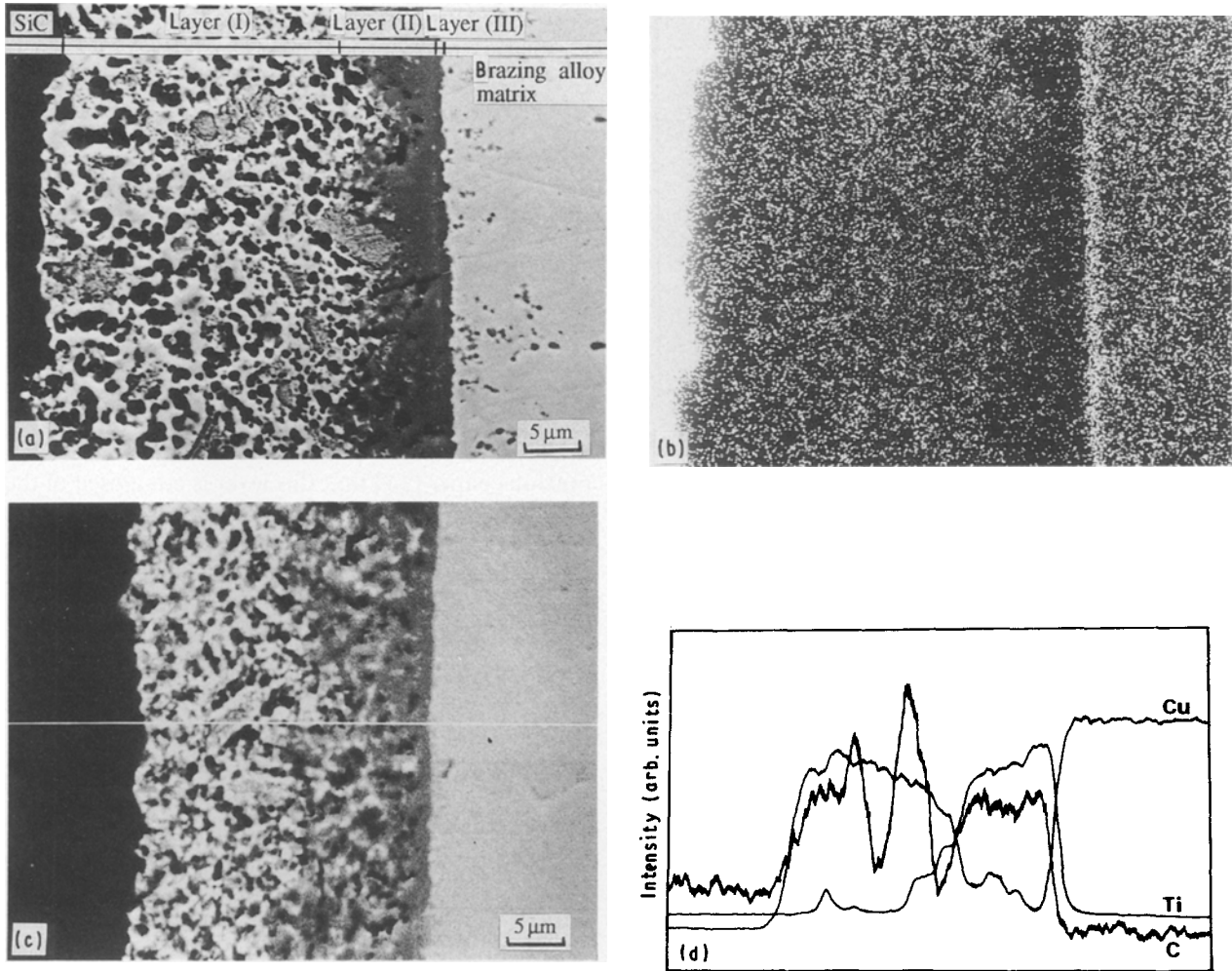
Figure 4 Microstructure and element distribution by the EDX at the interface of the brazements by the Cu–5 at % Ti alloy at 1100 °C for 600 s. (a) Microstructure, (b) distribution of silicon, (c) microstructure for line analysis, (d) line analysis of elements.
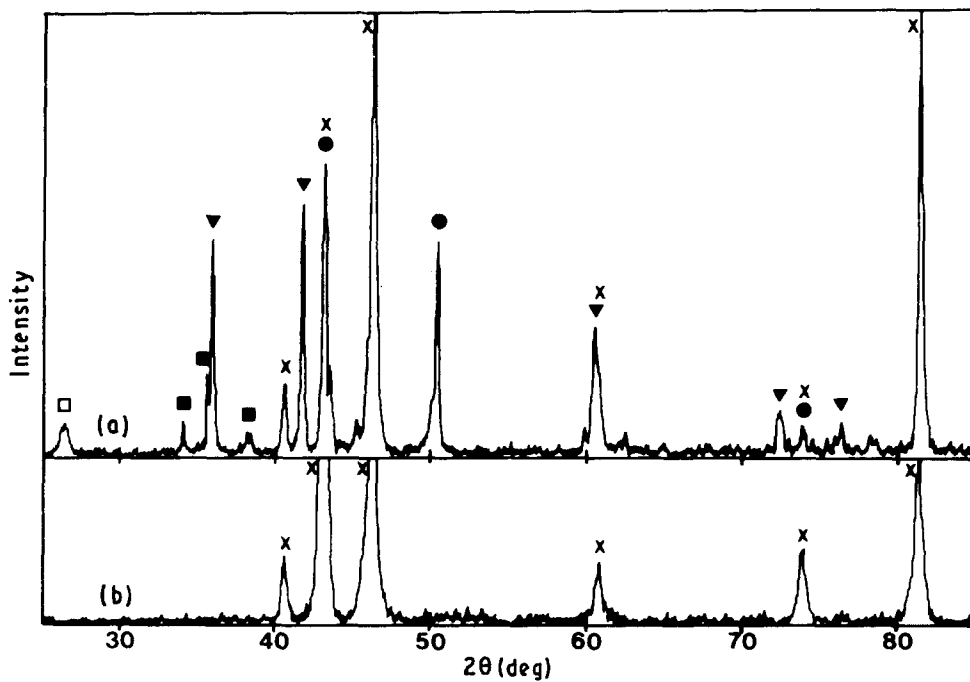

Figure 5 The result of XRD analysis for the specimen brazed by the Cu–5 at % Ti alloy at 1100 °C for 600 s, (a) for the reaction layers, (b) for the brazing alloy. (●) Cu, (■) SiC, (□) graphite, (▼) TiC, (×) Cu$_7$Si.

Figure 6 The reaction layers revealed after removing the brazing alloy by deep etching of the brazement by the Cu–5 at % Ti alloy at 1100 °C for 3600 s.

The brazing alloy matrix in brazing at 985 °C contained a small amount of titanium particles, changing all of titanium component in brazing at 1100 °C to the titanium silicides.

3.2.3. Ag_xCu_y–5 at % Ti alloy

Fig. 9 shows the microstructures and line analysis of the elements by EDX at the interface brazed by the $Ag_{0.6}Cu_{0.4}$–5 at % Ti alloy. The reaction layer seems to be a single layer. Decomposition of SiC was not found in brazing by this alloy. When brazed at 830 °C for 1800 s, the layer had a thickness of about 1 μm, as shown in Fig. 9a. On brazing at 830 °C for 600 s or at 920 °C for 600 s (Fig. 9c), the reaction layer had nearly the same microstructure as brazing at 830 °C for 1800 s with the exception of the difference in thickness of the reaction layer. Element distributions in Fig. 9b indicated that titanium has a peak intensity at the layer, but no carbon peak was found. The brazements by this alloy were easily separated through the boundary between SiC and the layer. XRD analysis on the brazing alloy matrix side of the separated surfaces was carried out. The result is shown in Fig. 10. TiC and Ti_5Si_3 were identified as the reaction products. XRD analysis after grinding out the reaction layer did not show any peak for TiC and Ti_5Si_3. Therefore, the reaction layer contains TiC and Ti_5Si_3. There was no peak of carbon in the layer because the TiC and Ti_5Si_3 phases coexist in the layer. Cu–Ti compounds that have the composition of 78.0Cu and 20.4 at % Ti from EDX analysis, were partially found in the brazing alloy matrix.

The Ti_5Si_3 phase from XRD analysis has directionality differing from that in the Ag–5 at % Ti alloy. Table II lists the intensity ratios of Ti_5Si_3 in comparison with JCPDS (Joint Committee on Powder Diffraction Standards) data. The peak intensities for the (0 0 2), (0 1 2) and (1 1 2) plane that have low angles with the (0 0 1) plane are increased in comparison with JCPDS data, while the peak intensities for the (1 2 0) and (1 2 1) plane that have high angles with the (0 0 1) plane are decreased. Thus the Ti_5Si_3 phase has grown preferentially in the normal direction of the (0 0 1)
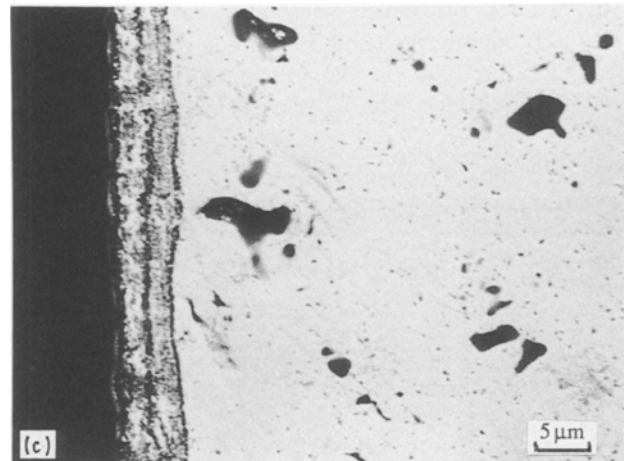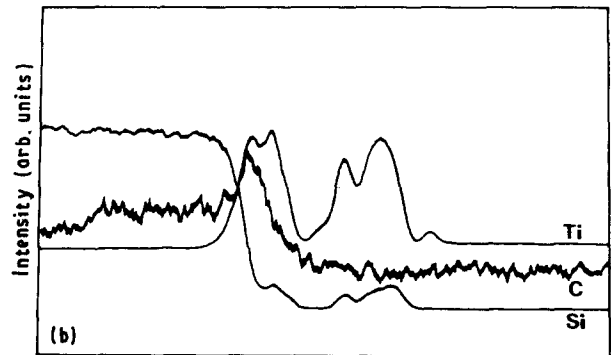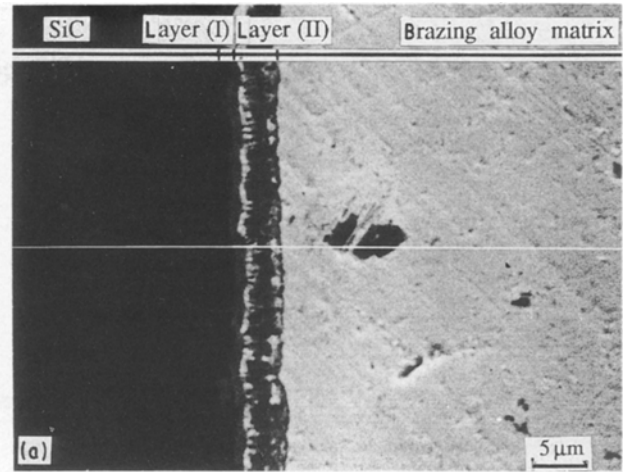

Figure 7 Microstructure and element distribution by EDX at the interface of the brazement by the Ag–5 at % Ti alloy at 985 and 1100 °C for 600 s. (a) Microstructure, 1100 °C/600 s; (b) element distribution; (c) microstructure, 985 °C/600 s.

plane. The preferential growth of Ti_5Si_3 was also observed in brazing by Cu–5 at % Ti alloy with a brazing gap of 0.4 mm at 1100 °C for 600 s [14].

Fig. 11a shows the microstructure at the interface when brazed by the $Ag_{0.1}Cu_{0.9}$–5 at % Ti alloy at 1100 °C for 600 s. The microstructure was nearly the same as the brazement by the Cu–5 at % Ti alloy with the exception of a small decrease in the thickness of the decomposition zone. Fig. 11b shows the microstructure of the brazement by the $Ag_{0.37}Cu_{0.63}$–5 at % Ti alloy at 890 °C for 600 s. The decomposition of SiC was observed at some interfacial regions. This brazement was easily separated through the interface.
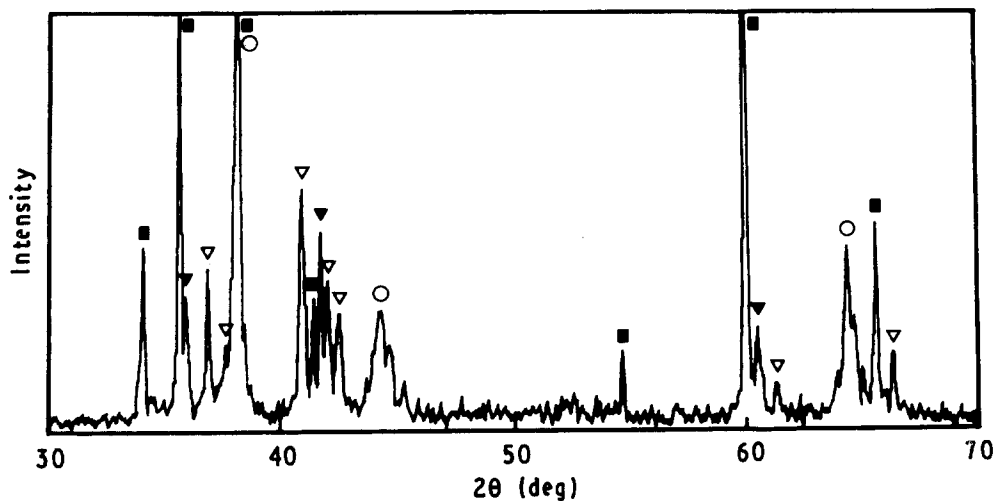
Figure 8 The result of XRD analysis on the reaction layers for the specimen brazed by the Ag–5 at % Ti alloy at 1100 °C for 600 s. (○) Ag, (■) SiC, (▼) TiC, (▽) Ti_5Si_3.

XRD analysis on the brazing alloy side of the separated surface showed that TiC and Ti_5Si_3 are produced as reaction products. Fig. 11c shows the microstructure of the brazement by the $Ag_{0.8}Cu_{0.2}$–5 at % Ti alloy at 980 °C for 600 s. There was no trace of the decomposition of SiC. The microstructure at the interface was similar to that in brazing by the Ag–5 at % Ti alloy. The reaction layers were divided into two layers and the brazing alloy matrix had penetrated between them. This brazement was also easily separated through the interface and TiC and Ti_5Si_3 were found by XRD analysis on the brazing alloy side of the separated surface. The Ti–Cu–Si compounds which

have the composition 75.7Ti–12.8Cu–11.8 at % Si from EDX analysis were found in the brazing alloy matrix.

3.3. Four-point bend test

Fig. 12 shows the results of the four-point tests on the specimens brazed by the Cu–5 at % Ti and Ag–5 at % Ti alloys. The scattering of the data is relatively small. The mean strength of 86 MPa was obtained in brazing by the Cu–5 at % Ti alloy. When brazed by the Ag–5 at % Ti alloy, the mean strengths of 159 MPa when brazing at 1100 °C for 600 s, and 178 MPa at 985 °C for 600 s were obtained. Almost all the specimens brazed by the $Ag_{0.6}Cu_{0.4}$–5 at % Ti, $Ag_{0.37}Cu_{0.63}$–5 at % Ti, and $Ag_{0.8}Cu_{0.2}$–5 at % Ti alloys failed through the interface during the preparation procedures of the specimens for the bend tests, and all have a bend strength lower than 20 MPa. The highest bend strength was found in brazing by Ag–5 at % Ti alloy at 985 °C for 600 s. The optimum brazing condition and composition would be different
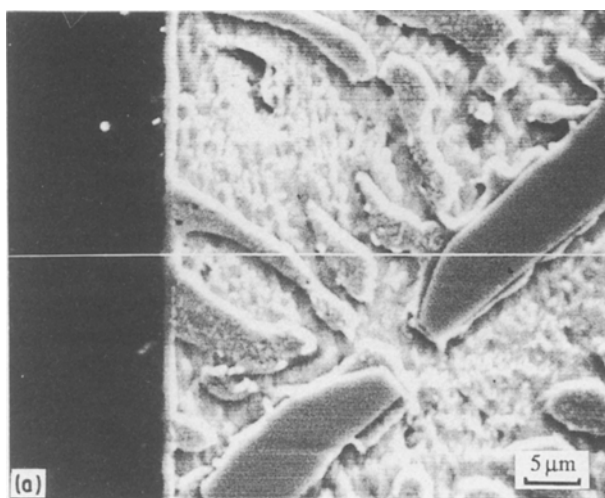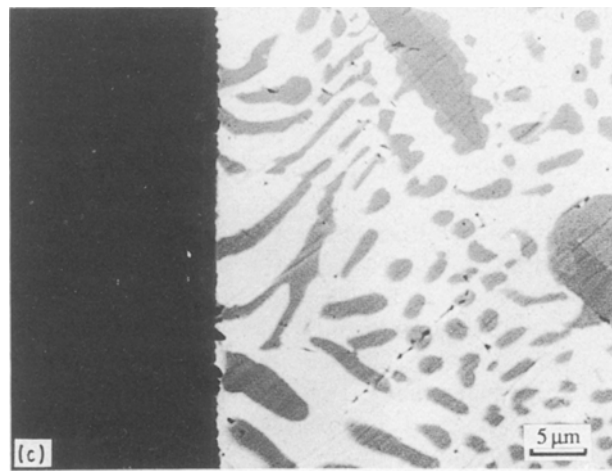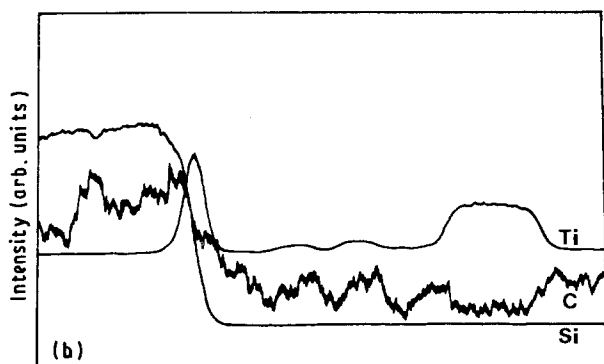

Figure 9 Microstructure and element distribution by EDX at the interface for the brazement by the $Ag_{0.6}Cu_{0.4}$–5 at % Ti alloy at 830 °C for 1800 s and at 920 °C for 600 s. (a) Microstructure, 830 °C/1800 s; (b) element distribution; (c) microstructure, 920 °C/600 s.
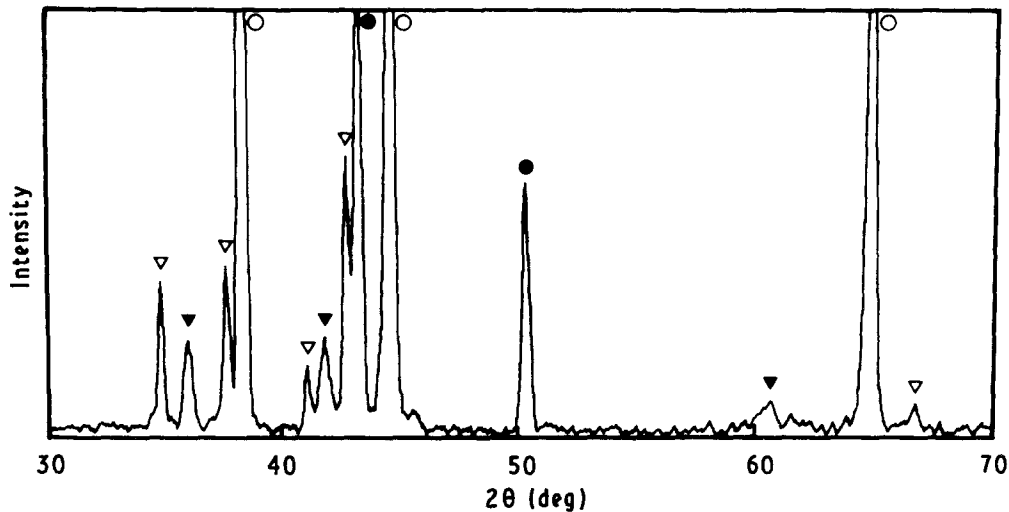
Figure 10 The result of XRD analysis on the brazing alloy side of the separated surfaces of the specimen brazed by the $Ag_{0.6}Cu_{0.4}-5$ at % Ti alloy at 830 °C for 600 s. (●) Cu, (○) Ag, (▼) TiC, (▽) Ti_5Si_3.
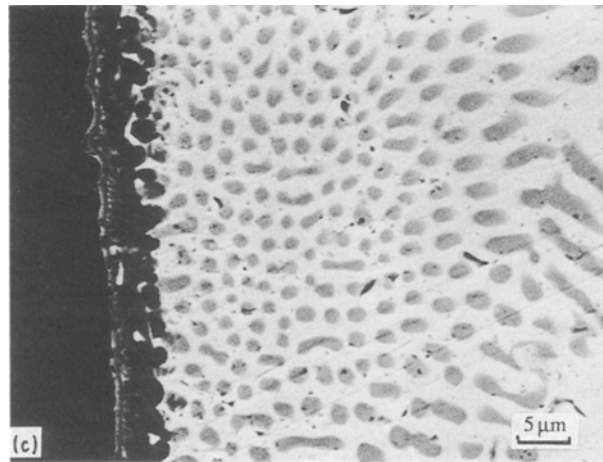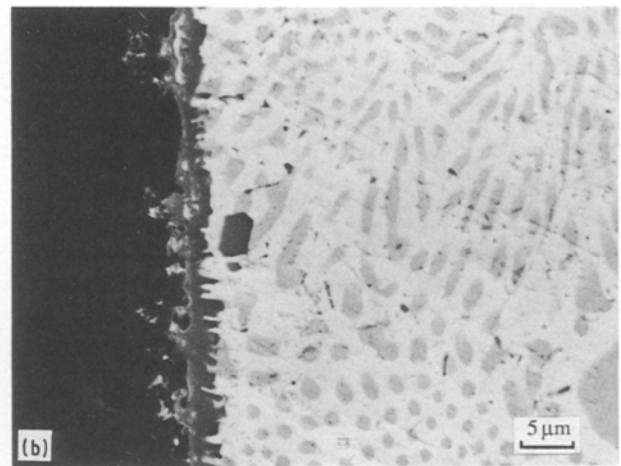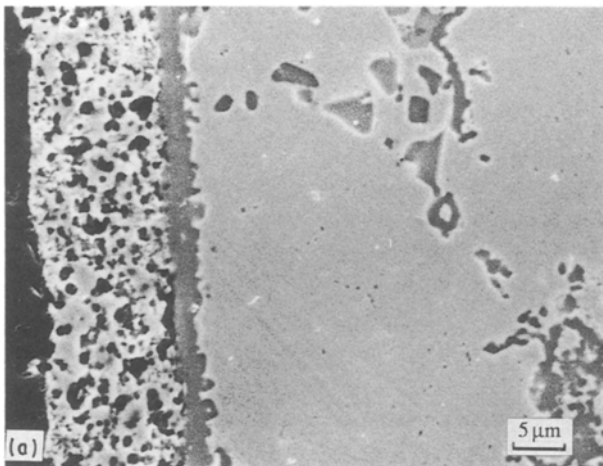

Figure 11 Microstructure at the interface of the brazement by the brazing alloys which deviated from the Ag–Cu eutectic composition. (a) $Ag_{0.1}Cu_{0.9}-5$ at % Ti alloy, 1100 °C/600 s; (b) $Ag_{0.37}Cu_{0.63}-5$ at % Ti alloy, 890 °C/600 s; (c) $Ag_{0.8}Cu_{0.2}-5$ at % Ti alloy, 980 °C/600 s.

with each alloy; therefore, it is difficult to compare the bend strength of the brazement by each alloy directly.

Fig. 13 shows the fracture surfaces after the bend tests. The failure modes differ greatly depending on the brazing alloys. Fig. 13a shows the fracture surface for the specimen brazed by the Cu–5 at % Ti alloy. Region A displays the fractured parts of SiC. Region B, which has the composition 89.7Cu–2.1Ti–8.2 at % Si from EDX analysis, is the Cu_7Si/graphite layer (reaction layer I in Fig. 4). Region C, which has the

composition 77.0Cu–13.3Ti–9.8 at % Si, is mainly constituted of the Cu_7Si/TiC layer (reaction layer II). Fractures initiate and propagate through SiC and the reaction layers. Fig. 13b shows the fracture surface for the brazement by the Ag–5 at % Ti alloy. Most fractures begin at the TiC layer and propagate through SiC in the rounded shape which is the typical failure mode in a good braze joint. Some fracture occurs through the boundary between SiC and the TiC layer. Fig. 14 shows the region of fracture initiation after the bend test. A plastically deformed band was observed in the brazing alloy matrix adjacent to the fracture surface and its position agreed well with the band of the Ti_5Si_3 phase (reaction layer II in Fig. 7). Fig. 13c shows the fracture surface in brazing by the $Ag_{0.6}Cu_{0.4}-5$ at % Ti alloy. Fractures initiate and propagate completely through the boundary between SiC and the reaction layer. The region marked A is magnified in Fig. 15, and the eutectic structure of the brazing alloy matrix was found between the fractured reaction layer. The fracture surfaces in the cases of the

TABLE II Comparison between the measured values and JCPDS data of the relative peak intensities for the lattice planes of Ti_5Si_3

Crystal plane	Angle with (0 0 1) plane (deg)	JCPDS		Cu–5Ti[a], 1100 °C/600 s		Ag–5Ti, 1100 °C/600 s		$Ag_{0.6}Cu_{0.4}$–5Ti, 830 °C/600 s	
		d(nm)	I/I_0	d(nm)	I/I_0	d(nm)	I/I_0	d(nm)	I/I_0
0 0 2	0	0.5571	10	0.25757	82	0.25652	14	0.25732	72
1 2 0	90	0.2436	35	0.24363	16	0.24364	71	0.24279	7
0 1 2	21.72	0.2388	18	0.23858	76	0.23903	31	0.23878	79
1 2 1	64.62	0.2202	100	0.22005	42	0.22033	100	0.21949	22
0 3 0	90	0.2149	40	TiC[b]	–	0.21464	56	TiC	–
1 1 2	34.61	0.2116	60	0.21161	100	0.21226	49	0.21127	100
2 2 2	54.07	0.1508	12	0.15053	8	0.15112	17	0.15052	9
1 2 3	35.10	0.1402	10	0.13993	8	0.14061	28	0.13987	13

[a] The results were calculated from the previous report [14] in which the specimen was brazed with the brazing gap of 0.4 mm.
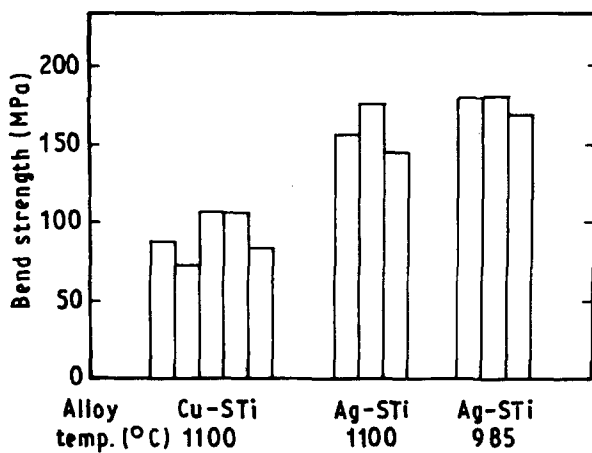[b] Overlapped with the peak from TiC which has high intensity.

Figure 12 Four-point bend strength of the specimens brazed by the Ag– and Cu–5 at % Ti alloy.

$Ag_{0.37}Cu_{0.67}$–5 at % Ti and $Ag_{0.8}Cu_{0.2}$–5 at % Ti alloys were very similar to that of the $Ag_{0.6}Cu_{0.4}$–5 at % Ti alloy.

4. Discussion

In brazing SiC by the silver- and copper-based active alloys, the microstructures at the interface differ from each other depending on the relative contents of silver and copper in the brazing alloy. The interfacial reactions can be divided into the decomposition reaction of SiC by the brazing alloy melt and the interfacial reaction of titanium with SiC. First the increase of copper content in the brazing alloy induces the decomposition of SiC by the brazing alloy melt. The reaction products from the interfacial reaction of titanium are TiC and Ti_5Si_3 in all the brazing alloys, but the morphology of the interface become different, depending on the relative contents of silver and copper in the brazing alloy.

The decomposition reaction of SiC can be explained by the activity of silicon in the copper and silver melt. The decomposition reaction of SiC can be expressed as

$$SiC(s) = Si + C(s), \quad \Delta G^0 = -RT \ln a_{si} \quad (1)$$

where Si indicates silicon solutionized in the copper and silver melt. It is shown in Fig. 16 that the activity

of silicon, a_{si}, changes with composition in each system [6, 7]. The solubility of silicon in the copper and silver melt can be calculated from the standard free energy change, ΔG^0, of the decomposition [7], if the temperature dependence of the activity of silicon in the copper melt is not as large in the low concentration range as in the silver melt. The activity of silicon at 1100 °C is calculated to be 0.029. The solubility of silicon in the copper and silver melt, which is obtained from Fig. 16, showed a large difference: about 18 and 1.5 at % Si, respectively. This means that SiC can be decomposed by the copper component in the Cu–5 at % Ti alloy melt, but decomposition is difficult by the Ag–5 at % Ti alloy melt. The decomposition reaction can be suppressed by the addition of silver in the Cu–5 at % Ti alloy and has been removed by the composition of $Ag_{0.6}Cu_{0.4}$–5 at % Ti.

The reaction products from the interfacial reaction of titanium are TiC and Ti_5Si_3 regardless of the system, but their distribution at the interface is affected by the relative contents of silver and copper in the brazing alloy. In the Cu–5 at % Ti alloy, carbon and silicon released from the decomposition of SiC react with titanium to produce TiC and Ti_5Si_3, as explained in detail in the literature [14]. The decomposition of SiC does not occur in brazing by the Ag–5 at % Ti and $Ag_{0.6}Cu_{0.4}$–5 at % Ti alloys. Therefore, titanium reacts with SiC directly. TiC and Ti_5Si_3 in the brazement by the Ag–5 at % Ti alloy are divided into discrete layers. In brazing by the $Ag_{0.6}Cu_{0.4}$–5 at % Ti alloy, they are contained in one layer, but Ti_5Si_3 has been grown with the preferred orientation, unlike TiC. From these results, it seems that TiC and Ti_5Si_3 in both cases have been produced sequentially. The formation mechanism of the titanium compounds can be explained as

$$SiC(s) + Ti = TiC(s) + Si \quad (2)$$

$$3Si + 5Ti = Ti_5Si_3(s) \quad (3)$$
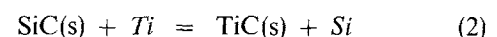
TiC is produced from the reaction between SiC and titanium in the brazing alloy melt (Equation 2) and then extra silicon reacts with titanium to produce Ti_5Si_3 (Equation 3). It is not understood why the distribution of TiC and Ti_5Si_3 in the brazements by the Ag–5 at % Ti and $Ag_{0.6}Cu_{0.4}$–5 at % Ti alloy differ from each other.
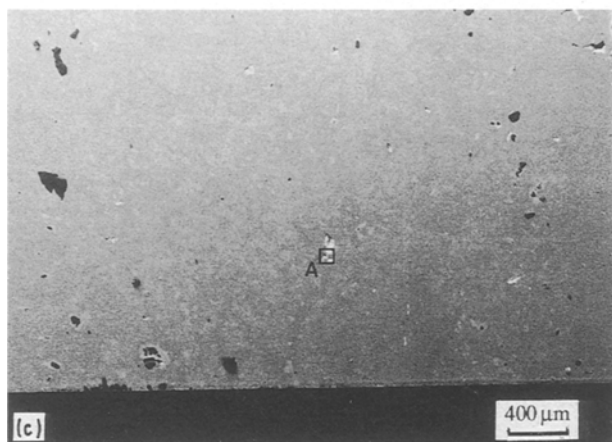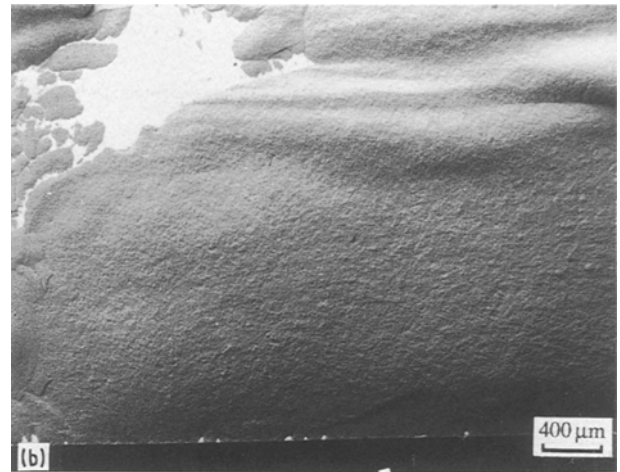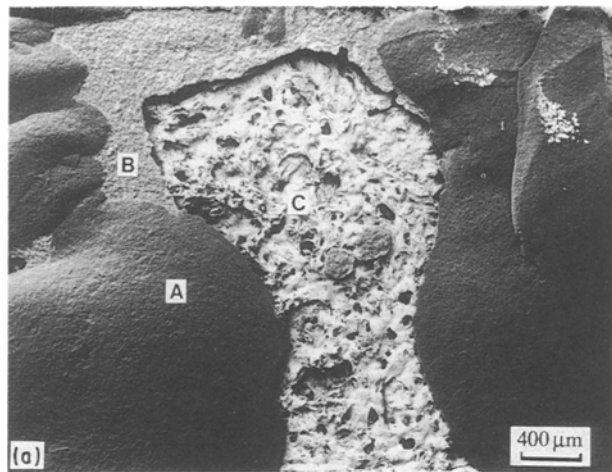
Figure 13 Fracture surfaces after the four-point bend tests for the brazements by each brazing alloy (fractures began from the bottom in the photographs). (a) Cu–5 at % Ti alloy, 1100 °C/600 s; (b) Ag–5 at % Ti alloy, 985 °C/600 s; (c) $Ag_{0.6}Cu_{0.4}$–5 at % Ti alloy, 830 °C/600 s.
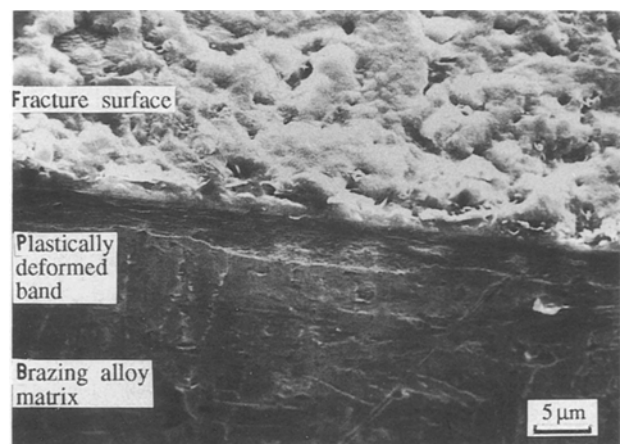

Figure 14 Plastic deformation band formed adjacent to the fracture surface in the four-point bend test of the brazement by the Ag–5 at % Ti alloy.
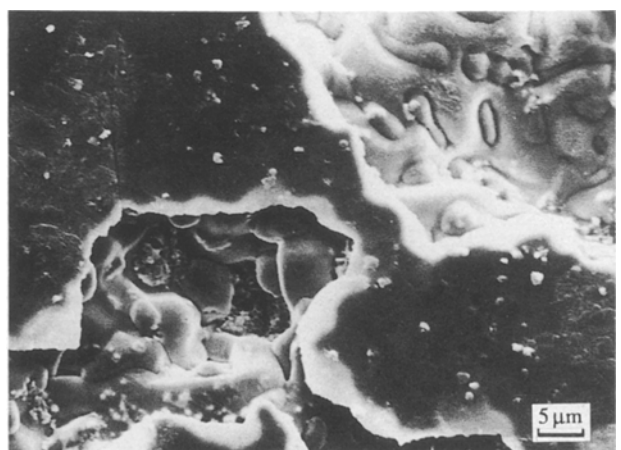

Figure 15 Ag–Cu eutectic structures shown between the fractured reaction layer (a region A in Fig. 13c).

The compositions of the particles distributed in the brazing alloy matrix are also different depending on the extent of the interfacial reactions and the content of copper in the brazing alloy. If silicon can be supplied sufficiently from the decomposition reaction, like the Cu–5 at % Ti alloy, titanium silicide particles are produced in the brazing alloy matrix. When the decomposition reaction has not occurred and the content of copper in the brazing alloy is high enough, as in the $Ag_{0.6}Cu_{0.4}$–5 at % Ti alloy, the Cu–Ti compounds are found in the brazing alloy matrix. In the case of the Ag–5 at % Ti alloy, there is no decomposition of SiC and no copper in the brazing alloy. Therefore, titanium silicide particles are produced or unmelted titanium particles remain. The Ti–Si–Cu compounds are produced in the brazing by the $Ag_{0.6}Cu_{0.2}$–5 at % Ti alloy which has a small amount of copper and cannot decompose SiC.

The braze joint by the Cu–5 at % Ti alloy has a four-point bend strength of 86 MPa. SiC is not contacted directly with TiC but contacted instead with the Cu_7Si/graphite composite layer. It is very difficult to obtain lattice matching between SiC and the Cu_7Si/graphite composite layer. Therefore, it is expected that this boundary will be weak. Fractograph in Fig. 13a shows that most of fractures propagate through this boundary and another weak boundary, the boundary between the Cu_7Si/graphite and Cu_7Si/TiC layers. It seems that the braze joint can have such a high bond strength because the

Cu_7Si/graphite composite layer has considerably relaxed the thermal stresses originating from the difference in the thermal expansion coefficient between SiC and the brazing alloy. The braze joint by the
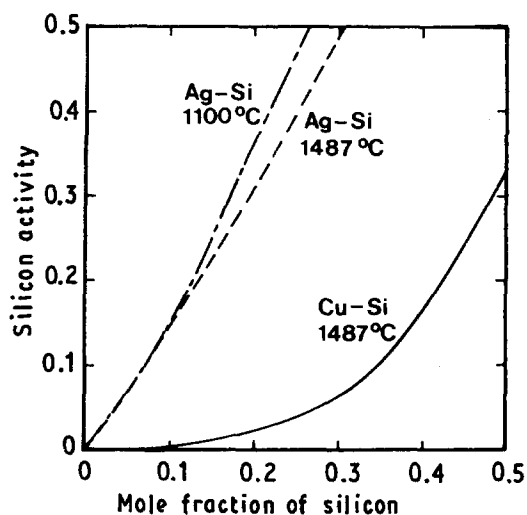
Figure 16 Activity of silicon in the copper and silver melt [6, 7].

Ag–5 at % Ti alloy has a good bond strength of 159–178 MPa. SiC is in direct contact with TiC. All of the lattice planes of TiC have similar interplanar distances to some lattice planes of SiC, as shown in the XRD analysis. Therefore, they can easily achieve a good lattice matching. The thermal stresses can be absorbed considerably because the silver matrix has a good ductility and the stress concentration at the interface can be relaxed because the Ti_5Si_3 layer is plastically deformed during the bend test, as shown in Fig. 14. From these facts, the braze joint by the Ag–5 at % Ti alloy can have high bond strength.

The braze joints by the $Ag_{0.6}Cu_{0.4}$–5 at % Ti alloy have very weak bond strengths and are fractured exactly through the boundary between SiC and the reaction layer. The weakness of the boundary can be caused by the distribution of Ti_5Si_3 phase in the reaction layer when compared with the case of Ag–5 at % Ti alloy. Backhaus-Ricoult [15] reported from experiments on the solid state reaction between SiC and titanium, that the reaction layer has the morphology of TiC precipitates in the Ti_5Si_3 matrix. If the reaction layer in this system has similar morphology, it is difficult to have a good lattice matching between SiC and the reaction layer. On the contrary, other researchers [5] have reported from similar brazing experiments to this system, with the exception of the use of tantalum heater, that some lattice planes of TiC are well matched with those of SiC. They have also insisted that TiC phase was found in the reaction layer adjacent to SiC, while Ti_5Si_3 phase was found in the remote area from the reaction layer. More research on the detailed morphology of the reaction layer is required to confirm the causes of the weakness of the boundary in the brazing by the $Ag_{0.6}Cu_{0.4}$–5 at % Ti alloy.

It has been proved from this research that the relative contents of silver and copper in the brazing alloy affect the interfacial reactions and bond strength in the active metal brazing of SiC. The optimum brazing conditions should be designed with consideration of the microstructure for each brazing alloy in such a way as to obtain a good bond at the interface with SiC and to reduce the thermal stresses.

5. Conclusions

In the brazing of SiC by Cu–5 at % Ti, Ag–5 at % Ti, and Ag_xCu_y–5 at % Ti alloys, the microstructure at the interface, bond strength and fracture mode differ depending on the relative contents of silver and copper in the brazing alloy.

1. In the brazing of SiC by Cu–5 at % Ti alloy, SiC is easily decomposed by the copper melt. Graphite and silicon released from the decomposition reacts with titanium to produce TiC and Ti_5Si_3, respectively. The decomposition of SiC is suppressed by the addition of silver in the brazing alloy, and disappeared in the $Ag_{0.6}Cu_{0.4}$–5 at % Ti to Ag–5 at % Ti alloy.

2. TiC in brazing by the Ag–5 at % Ti alloy is formed as a thin layer in contact with SiC, while Ti_5Si_3 is formed as a sparse band independent of the TiC layer. TiC and Ti_5Si_3 in brazing by the $Ag_{0.6}Cu_{0.4}$–5 at % Ti alloy coexist in one layer, but Ti_5Si_3 grows with a directionality.

3. A bond strength of 86 MPa was found in the brazement by the Cu–5 at % Ti alloy from four-point bend tests, and fracture is initiated and propagated through SiC and the reaction layers. The brazement by the Ag–5 at % Ti alloy has a bond strength of 159–178 MPa, depending on the brazing temperature, and fracture is initiated at the boundary between SiC and the TiC layer and mostly propagates through SiC. The braze joint by the $Ag_{0.6}Cu_{0.4}$–5 at % Ti alloy is very weak and fractures through the boundary between SiC and the reaction layer.

Acknowledgement

References

1. T. OKUO, Y. KUSAKA and Y. AIYAMA, *J. High Temp. Soc.* **11** (1985) 186 (in Japanese).
2. T. W. EAGAR, *Weld. J.* **66** (1987) 35.
3. H. MIZUHARA and E. HUEBEL, *ibid.* **65** (1986) 43.
4. J. K. BOADI, T. YANO and T. ISEKI, *J. Mater. Sci.* **22** (1987) 2431.
5. T. YANO, H. SUEMATSU and T. ISEKI, *ibid.* **23** (1988) 3362.
6. H. SAKAO and J. F. ELLIOTT, *Metall. Trans.* **5** (1974) 2036.
7. O. KUBASCHEWSKI and C. B. ALCOCK, "Metallurgical Thermochemistry" (Pergamon Press, Oxford, 1979).
8. G. G. GNESIN and YU. V. NAIDICH, *Sov. Powder Met. Metal Ceram.* **74** (1969) 128.
9. V. N. EREMENKO, YU. I. BUYANOV and N. M. PANCHENKO, *ibid.* **89** (1970) 410.
10. J. A. PASK, *Amer. Ceram. Soc. Bull.* **66** (1987) 1587.
11. D. A. MORTIMER and M. NICHOLAS, *J. Mater. Sci.* **8** (1973) 640.
12. T. ISEKI, T. YANO and Y. S. CHUNG, *Jpn Ceram. Soc. Bull.* **97** (1989) 710 (in Japanese).
13. A. J. MOORHEAD and H. KEATING, *Weld. J.* **65** (1986) 17.
14. H. K. LEE and J. Y. LEE, *J. Mater. Sci. Lett.* **11** (1992) 550.
15. M. BACKHAUS-RICOULT, in "Proceedings of the International Workshop on Bonding, Structure, and Mechanical Properties of Metal/Ceramic Interfaces", Santa Barbara, January 1989, edited by M. Rühle, A. G. Evans, M. F. Ashby, J. P. Hirth (Pergamon Press, Oxford, 1990) p. 79.